Range filters: local-intensity subrange filters and their properties

D G Bailey and R M Hodgson

A local filter which uses the local-intensity subrange of pixel intensity values within a window is described. The range filter is an extension of the rank filter and has been found useful for detecting edges. The deterministic and noise properties of the range filter are described and compared with those of the commonly used Sobel filter.

Keywords: range filters, rank filters, local filters, edge detection

In image processing, a local filter is any operator whose output for a pixel is a function of the input values within the neighbourhood of that pixel[1]. This neighbourhood can be thought of as a window, which is scanned across the input image; each position contributes one pixel to the output image. The window can be of any shape, although it is almost always symmetrical about a centre pixel[2] and is usually square. Local filters tend to have short calculation times, since generally only a small number of input pixels are operated on for each output pixel.

A local subrange filter uses the statistical subrange of the pixel intensities within the window. In this paper, this filter is referred to as the range filter. The range and interquartile distance are often used in statistics as a measure of the variation of a sample. The interquartile distance has been applied to image processing by Scollar *et al.*[3], as a substitute for the standard deviation, as a measure of the variation of pixel intensities within a window. If a region has very little spread in the local intensity values, then the range and interquartile distance are small. If a region has large discontinuities in intensity, or is very noisy, the local range and interquartile distance are large. One of the features of interest to those who use image processing is edges. Since edges are typically characterized by discontinuities in mean intensity[4], range filters will detect edges. This paper investigates the effectiveness of these filters for this task.

University of Canterbury, Private Bag, Christchurch, New Zealand

The local subrange is calculated by ordering the N pixels within the window according to intensity, ie

$$(f_1, f_2, f_3, \ldots, f_N) \tag{1}$$

where

$$f_1 \leqslant f_2 \leqslant \cdots \leqslant f_N \tag{2}$$

and then subtracting the intensity values for two selected positions (i and j) within this ordered list such that

$$\mathrm{range}(j,i) = f_j - f_i \qquad 1 \leqslant i < j \leqslant N \tag{3}$$

When this is performed over the whole image, it may be represented by

$$g = \mathrm{Ra}_{j,i}(f) \tag{4}$$

where g is the output image. Thus the range filter is an extension of another local nonlinear filter, the rank filter[5], defined as

$$\mathrm{rank}(i) = f_i \qquad 1 \leqslant i \leqslant N \tag{5}$$

When performed over the whole image, this may be represented by

$$g = R_i(f) \tag{6}$$

Therefore, combining equations (3)–(6) gives

$$\mathrm{Ra}_{j,i}(f) = R_j(f) - R_i(f) \qquad i < j \tag{7}$$

Thus a range-filtered image is the difference of two rank-filtered images. Some of the properties of the range filter may be derived from the properties of the rank filter. Rank filters shift edges between regions of different intensity[6,7]. If two rank filters are used with different positions in the sorted list being selected, the edge will be moved by differing amounts. The difference between these, ie the local subrange, will represent edge activity[5]. This concept of shifting the edges and detecting the change that occurs has been discussed by Goetcherian[7] and Pal and King[8]. They used one or other of the processes represented by

$$g = f - \text{rank } 1 \tag{8a}$$

$$g = \text{rank } 9 - f \tag{8b}$$

BENCHMARK SELECTION

The shifting of edges followed by the subtraction of the original image is a form of differentiation. In Figures 1a–1c, the response of a one-dimensional two-element range filter to a step edge and to an impulse are compared with the first difference. The range filter will always give a positive response for real data, since the pixel values are ordered before subtraction. When a range filter with a larger window is used, the responses become even more different from the first difference (see Figures 1d–1f). In some cases, some pixel values may never be selected as the window is scanned past. This is demonstrated in Figure 1e by the impulse response of a three-element range 2,1 filter. For the two-dimensional range filter, the relationship with differentiation is even more subtle since the two pixel values that are subtracted to give the output may come from anywhere within the window.

The properties and usefulness of the range filter can be illustrated by comparing it with the commonly used Sobel filter. The Sobel filter is a local filter which performs two-dimensional differentiation[4]. This filter consists of two linear filters which perform differentiation in the horizontal and vertical directions. The outputs of these filters are combined according to

$$g = \frac{\partial f}{\partial x}\mathbf{i} + \frac{\partial f}{\partial y}\mathbf{j} \tag{9}$$

to give a two-dimensional differential response. The weights used for the components of the Sobel filter[9] are given by

$$\mathbf{D}_x = \tfrac{1}{4}\begin{vmatrix} -1 & 0 & 1 \\ -2 & 0 & 2 \\ -1 & 0 & 1 \end{vmatrix} \qquad \mathbf{D}_y = \tfrac{1}{4}\begin{vmatrix} 1 & 2 & 1 \\ 0 & 0 & 0 \\ -1 & -2 & -1 \end{vmatrix} \tag{10}$$

The magnitude of equation (9) gives the gradient, making the resultant image

$$g = [(\mathbf{D}_x \odot f)^2 + (\mathbf{D}_y \odot f)^2]^{1/2} \tag{11}$$

where $\odot$ denotes convolution and the square and square root are defined as pixel operations. To simplify the computation, the forms

$$g = |\mathbf{D}_x \odot f| + \mathbf{D}_y \odot f| \tag{12}$$

$$g = \max(|\mathbf{D}_x \odot f|, |\mathbf{D}_y \odot f|) \tag{13}$$

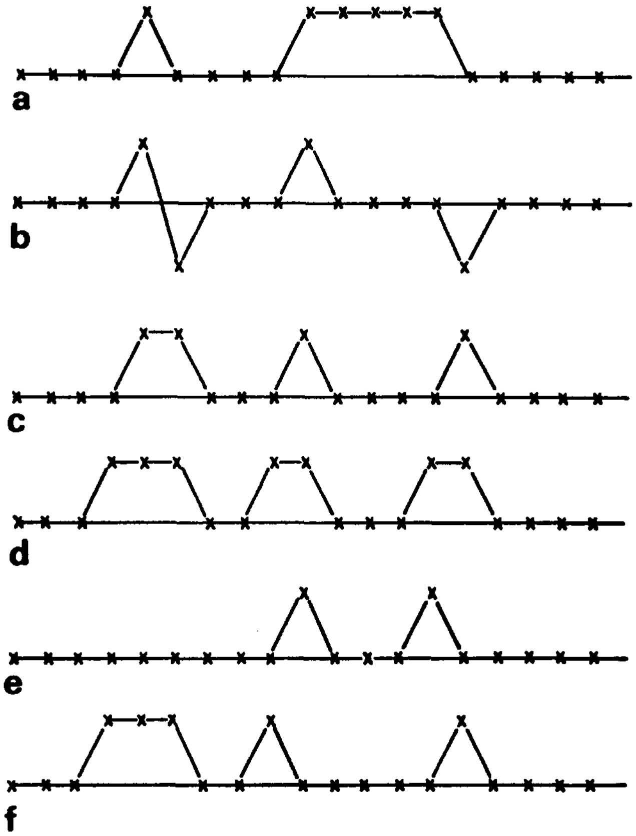

Figure 1. Differential nature of range filters: **a** *original one-dimensional image consisting of an impulse and two steps;* **b** *the first difference of* **a**; **c** *response of a two-element range filter (range 2,1);* **d–f** *responses of the three different three-element range filters (range 3,1; range 2,1; and range 3,2 respectively)*

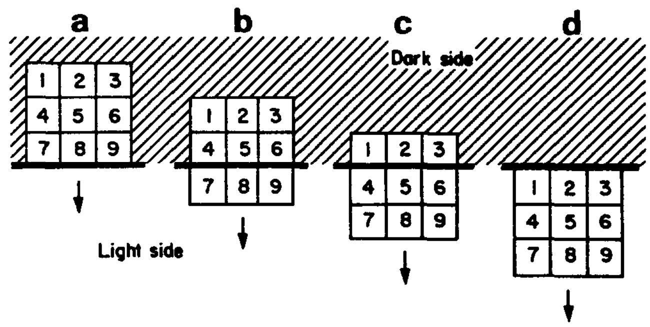

Figure 2. Response of a range filter using a 3 × 3 square window as the window approaches a horizontal edge; **a** *no window positions respond;* **b** *window positions 7–9 respond;* **c** *window positions 4–9 respond;* **d** *all positions respond*

Table 1. Width of the response of 3×3 square range filters to horizontal or vertical edges

i \ j	9	8	7	6	5	4	3	2
1	2	2	2	1	1	1	0	0
2	2	2	2	1	1	1	0	
3	2	2	2	1	1	1		
4	1	1	1	0	0			
5	1	1	1	0				
6	1	1	1					
7	0	0						
8	0							

are often used[4] (max is defined as a pixel operation).

The Sobel filters defined by equations (11)–(13) are used below as a benchmark for the range filters.

EFFECT OF RANGE FILTERS ON BINARY IMAGES

The edge detection properties of range filters can be illustrated using noiseless images of binary edges. (The effect of noise on range filters will be discussed below.) This section considers the response of range filters to the boundaries between adjacent black and white regions. A 3×3 square window is used unless otherwise specified.

Response to horizontal and vertical edges

The response of a 3×3 square range filter is the same for both vertical and horizontal edges, since the window is rotationally symmetric. The width of the response to horizontal or vertical edges is shown in Table 1. The blocked nature of the response among the different range filters arises from the shape of the window, and the way the window crosses the edge. Figure 2 shows that, as the window approaches the edge, window positions 7–9 respond simultaneously, as do window positions 4–6 and 1–3. The physical spacing within the window between the two rank positions used in the range filter determines the width of the detected edge. The two component rank filters shift the edge by different amounts, allowing the width and position of the detected edge to be specified in the output image by selecting appropriate rank values.

Response to 45° diagonal edges

The width of a diagonal edge response can be defined as the horizontal width of the response in pixels (Figure 3). The response of range filters to diagonal edges is listed in Table 2, and may be determined in a similar way to that for horizontal and vertical edges (see Figure 4).

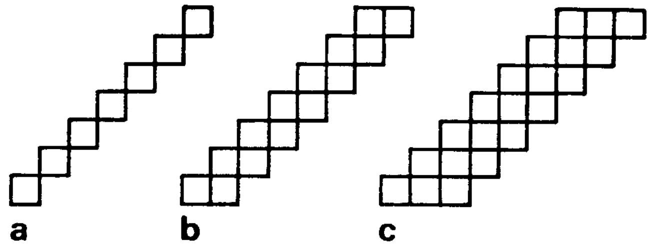

Figure 3. Definition of the width of a diagonal edge: **a** *a single-pixel-width edge;* **b** *a two-pixel-width edge;* **c** *a three-pixel-width edge*

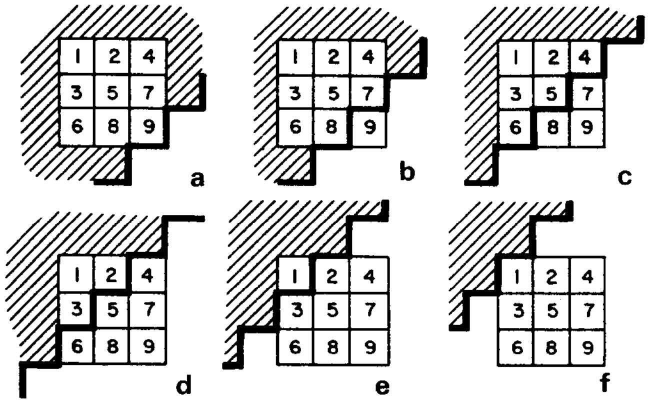

Figure 4. Response of a range filter using a 3×3 square window as the window approaches a diagonal edge: **a** *no window positions respond;* **b** *window position 9 responds;* **c** *window positions 7–9 respond;* **d** *window positions 4–9 respond;* **e** *window positions 2–9 respond;* **f** *all window positions respond*

Detected edge width

The width of the detected edge is often important. Filters with a response of one-pixel width are ideal if the response is on the desired side of the edge. In this case no thinning is required to obtain an edge map. The desired side of the edge is determined by the processing that is to take place after edge detection. This may be important if area or size measurements are to be made using the detected edge to represent the boundary of the object. By selecting the parameters of the range filter, the response may be positioned on the light or the dark side of the actual edge. To get a similar result by thinning a wider response would involve unnecessary complications in the thinning algorithm, since information has been lost as to which side of the edge is the light or dark side. A single-pixel-width response may be a disadvantage when the image is noisy, since it is likely that some of the edge points will not be detected. This results in breaks in the output image and further processing is then needed to fill them.

When uncertainty exists as to whether the response should be positioned on the light or dark side of the edge, an output two pixels wide is useful. In this case it is desirable to generate one pixel on each side of the original edge, so that the true edge is then the centre of response. A two-pixel-width response is also less susceptible to noise because, if some edge points are not detected, these are less likely to result in complete breaks in the output response.

Responses wider than two pixels are only useful when the image is noisy to the extent that the edges are not detected reliably with a narrower response. In this case, algorithms are required to connect and thin the edges that are detected. The main disadvantage of a wide response is a cluttering of the image with detected edge points, especially when processing low-resolution images.

The Sobel filter gives a two-pixel-width response to

Table 2. Width of the response of 3×3 square range filters to 45° diagonal edges

i \ j	9	8	7	6	5	4	3	2
1	4	3	3	2	2	2	1	1
2	3	2	2	1	1	1	0	
3	3	2	2	1	1	1		
4	2	1	1	0	0			
5	2	1	1	0				
6	2	1	1					
7	1	0						
8	1							

both horizontal and vertical edges and a response two or four pixels wide to diagonal edges of 45° (depending on the threshold used). This behaviour is similar to the response of the 3 × 3 square range filter using range 9,1 or range 8,2. The general advantage of the range filters is that the width of the response can be selected by parameter selection.

Response to general diagonal edges

When the angle of a diagonal edge is other than 45°, the edge appears as a series of quantized horizontal or vertical 'steps' as shown in Figure 5. The properties of a range filter in the vicinity of these steps determine the response to diagonal edges. For this reason, an isolated step will be considered. Away from the step, the response is the same as that listed in Table 1 for a horizontal or vertical edge. The characterizing feature of the response to the step is therefore the overlap that occurs between the responses of the filter to the horizontal or vertical sections on either side of the step. This overlap will be defined as the number of pixels along the direction of the edge for which the response is wider than that in the absence of the step. Examples of different overlaps are shown in Figure 6. Table 3 shows the overlap for the range filters considered.

The overlap may be calculated by considering the number of pixels on the light side of the edge as the window approaches the step. Figure 7 shows the case for the 3×3 square window. The pixels that are selected by the range filter are those that are less than the higher rank position, and greater than or equal to the lower rank position. Thus the overlap is given by the distance, along the edge, between the first occurrence of the numbers corresponding to the two rank positions being used. The first occurrence of the numbers corresponding to each rank position falls within the window shape rotated through 180°, since rank and range filtering are convolution-like operators in that the window is scanned across every pixel position. This is shown more clearly in Figure 8 for an asymmetrical window shape. The overlap is therefore given by the difference in position in the window. For example, with a 3 × 3 square window, the difference in position between ranks 3 and 7 is −2 (see also Figure 7).

Connectivity

The importance of the overlap is seen when the connectivity between the adjacent pixels in the output image is considered. With a rectangular sampling grid, there are two main pixel connectivity schemes[10]:

Table 3. Overlap in the response of 3 × 3 square range filters to non-45° diagonal edges

i \ *j*	9	8	7	6	5	4	3	2
1	2	1	0	2	1	0	2	1
2	1	0	−1	1	0	−1	1	
3	0	−1	−2	0	−1	−2		
4	2	1	0	2	1			
5	1	0	−1	1				
6	0	−1	−2					
7	2	1						
8	1							

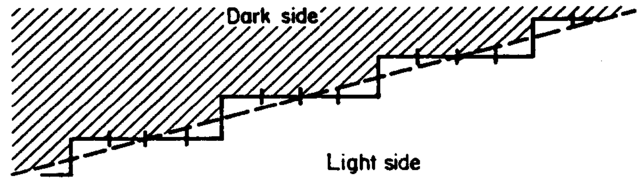

Figure 5. The stepped nature of a non-45° diagonal edge

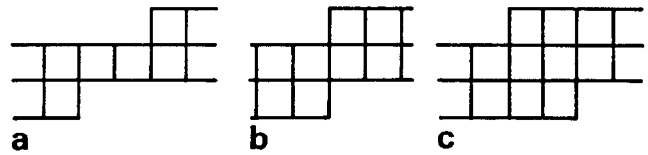

Figure 6. Definition of overlap in the response to a non-45° diagonal edge: **a** *overlap is −2;* **b** *overlap is 0;* **c** *overlap is 2*

0	0	0	0	0	0	0
0	0	1	2	3	3	3
3	3	4	5	6	6	6
6	6	7	8	9	9	9
9	9	9	9	9	9	9

Figure 7. Graphical calculation of the overlap caused by a range 7,3 filter. (Ra 7,3 has an overlap of −2 since 7 is two squares to the left of 3.) The numbers in the squares indicate the number of rank positions within the window that respond as the window approaches the edge. The first occurrences of each number are boxed

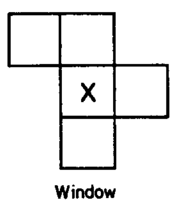

0	0	0	0	0	0	0
0	0	0	1	1	1	1
1	1	2	3	3	3	3
3	3	3	4	5	5	5
5	5	5	5	5	5	5

Figure 8. Rotation of the window through 180° in the first occurrences of the numbers of rank positions that respond

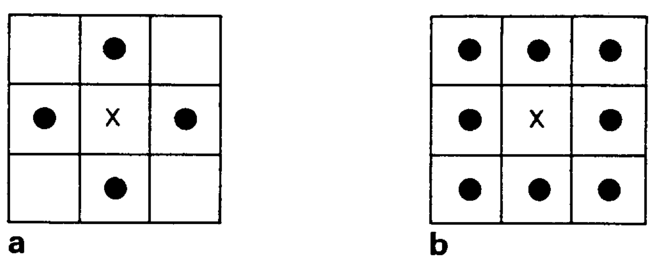

Figure 9. Definition of the two common neighbourhood schemes on rectangular grids: **a** *4-connected neighbours;* **b** *8-connected neighbours*

4-neighbour and 8-neighbour connectivity. The 4-neighbour scheme allows a pixel to be connected to its four neighbours in the horizontal and vertical directions. The 8-neighbour scheme allows the four diagonal neighbours to be used in addition to the four horizontal and vertical neighbours. These two schemes are illustrated in Figure 9. Corresponding to these two connectivity schemes, there are two chain coding schemes for the resultant edges[11]. Coding may be simplified if the connectivity of the detected edges corresponds to the connectivity of the chain code. This is really only important when the width of the detected edge is a single pixel, since wider edges can be thinned before they are coded. Range filters can be used to give responses corresponding to either connectivity scheme by selecting appropriate parameters.

To obtain a consistent response to 45° diagonal edges and to other diagonal edge directions when using the 4-neighbour scheme, it is necessary (in addition to having a single-pixel overlap on steps) that the response to diagonal edges at 45° should also be two pixels wide (eg range 5,1 or range 9,5). Similarly, when the 8-neighbour scheme is used, the desired response to 45° diagonal edges will be a single pixel wide (eg range 5,2; range 6,3; range 7,4; and range 8,5).

Dependence of the response on window shape and size

The response of range filters to noiseless binary edges differs considerably from one window shape to another, as illustrated by comparing the horizontal edge response of a 3 × 3 square window (Table 1) and that of a nine-element cross window (Table 4). The use of asymmetric windows will not be considered here, although they may be useful in detecting edges of a specific shape or orientation. The lack of symmetry makes them of little use as general edge detectors. Windows larger than those discussed here give wider responses. The main effect of changing the window size is to scale the response. The window shape has a marked effect on the response to binary edges. This is because the interaction between the window and the edge depends primarily on the window shape, as demonstrated by comparing the responses of the 3 × 3 square window and the nine-element cross window.

Comparison with the Sobel filter

As mentioned above, the response of the Sobel filter is similar to that of the range 9,1 or range 8,2 filters. Range filters have the advantage of being able to specify the width and position of the output. In low-noise applications, this ability may be useful since it avoids the need to thin the resultant edge map in order to code the edge. Range filters have the added advantage that the connectivity of the resultant edge can be specified for filters with a single-pixel-width response.

A disadvantage of the Sobel filter is that, with binary images, the output is almost always many valued. To obtain a binary edge map, the output image requires thresholding. Although this will be necessary in any case for greyscale images, it is an extra step when the image is already in binary form. In general, for range

Table 4. Width of the response of nine-element cross range filters to horizontal or vertical edges

i \ j	9	8	7	6	5	4	3	2
1	4	3	2	2	2	2	2	1
2	3	2	1	1	1	1	1	
3	2	1	0	0	0	0		
4	2	1	0	0	0			
5	2	1	0	0				
6	2	1	0					
7	2	1						
8	1							

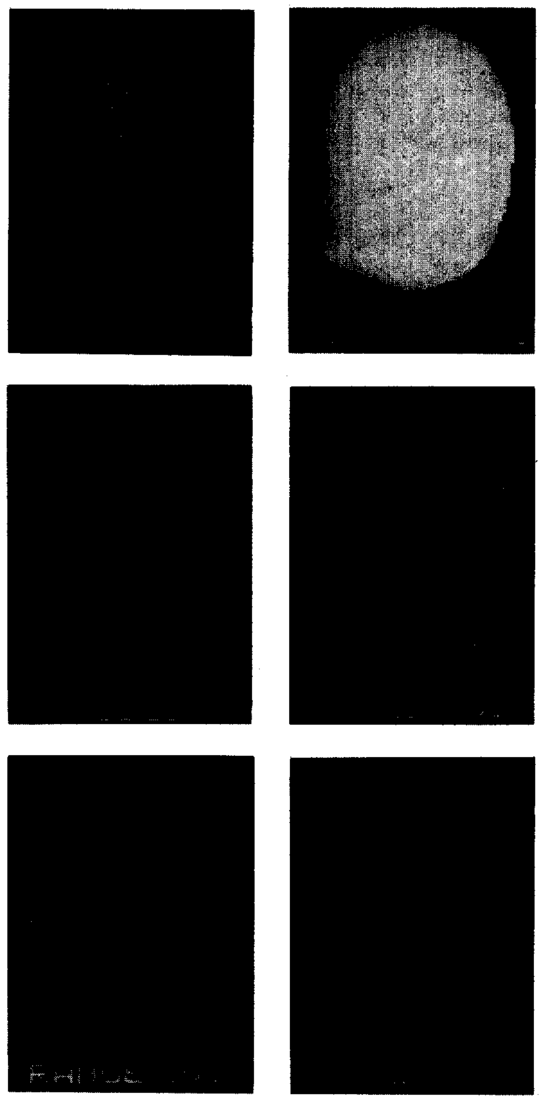

Figure 10. The use of range filters to determine the outline of kiwi fruit images. An image of a kiwi fruit with a defect known as 'Hayward mark' is processed by the Sobel and range 9,1; 9,5; and 8,5 filters

filters that are useful as general edge detectors, the parameters of the constituent rank filters differ by more than two.

Rather than compare the response of every range filter with that of the Sobel filter, only two or three range filters will be used. These filters are chosen to illustrate the variety of responses available from the range filters in different situations.

An example of the successful use of range filters is the extraction of the outline of kiwifruit in a shape-defect-detection algorithm. A silhouette image is simply filtered with a range filter. The different connectivity schemes of the resultant line image produced by the range 9,1, range 9,5 and range 8,5 filters are demonstrated in Figure 10. The image is then chain coded and the resultant chain code is processed to determine whether the fruit is defective.

RESPONSE TO A UNIFORM INTENSITY GRADATION

Since the range filter is a type of differentiating filter, the output depends on the intensity slope within a region, as well as on discontinuities in intensity. In the following discussion of the direction dependence of the response of range filters, a local region of uniform intensity slope is used as a test (see Figure 11). The centre element is normalized to 0 and the slope amplitude is normalized to 1. The slope is a multiplicative constant and only has an effect when a limited number of discrete intensity steps is used. It is assumed

$\cos\alpha$ $-\sin\alpha$	$\cos\alpha$	$\sin\alpha$ $+\cos\alpha$
$-\sin\alpha$	0	$\sin\alpha$
$-\sin\alpha$ $-\cos\alpha$	$-\cos\alpha$	$\sin\alpha$ $-\cos\alpha$

Figure 11. The normalized intensities within a 3×3 window when a uniform slope is being filtered

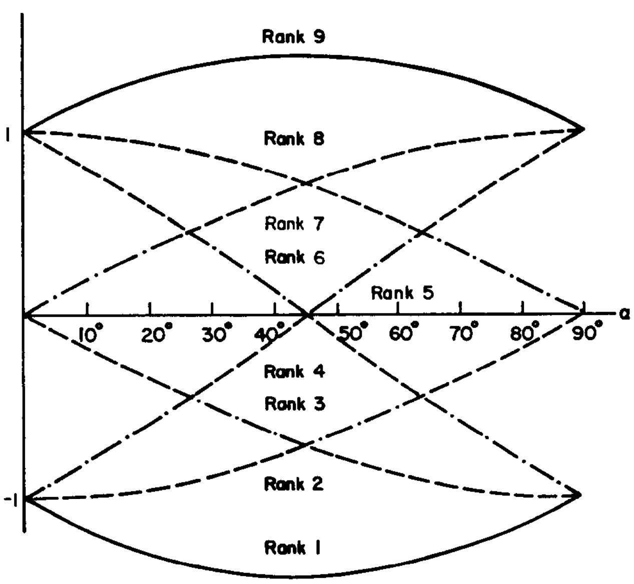

Figure 12. The dependence of ranked normalized intensities within a 3×3 window when a uniform slope is being filtered, versus the direction of the slope

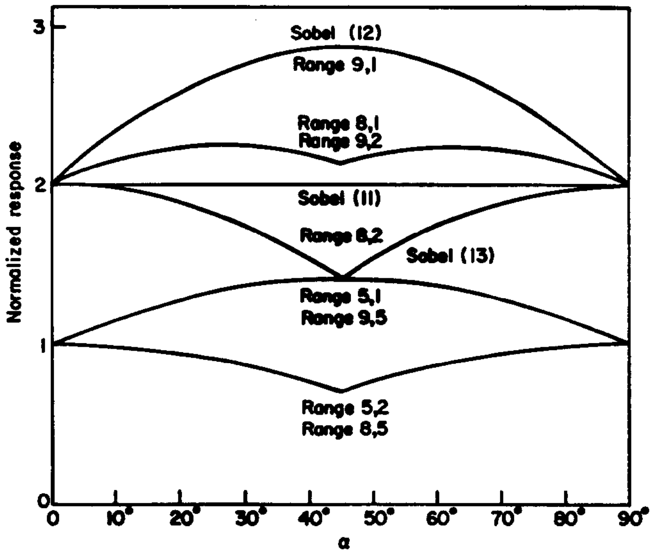

Figure 13. The normalized responses of selected range filters and Sobel filters when filtering a uniform slope, showing the directional dependence of the various filters

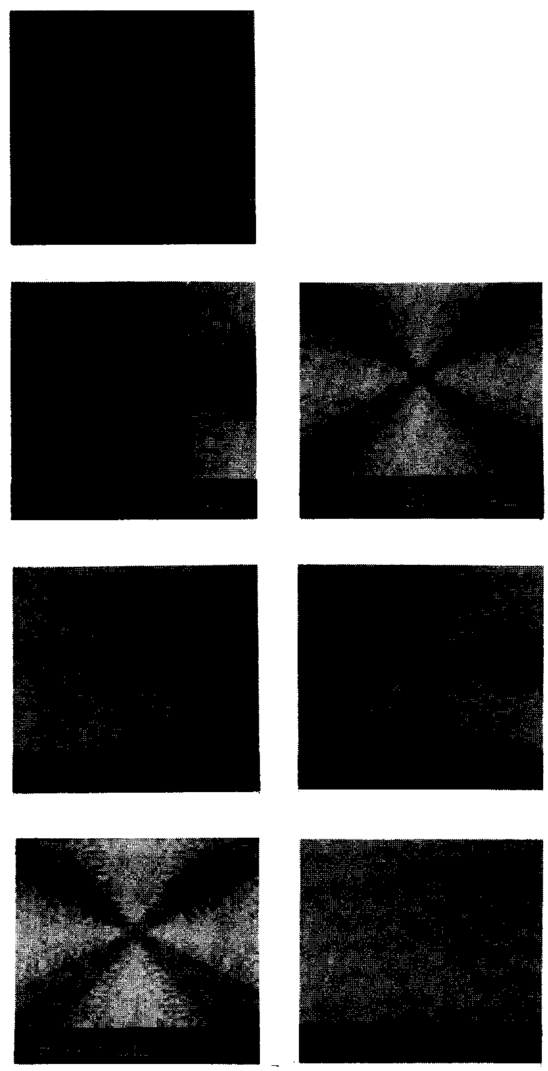

Figure 14. Normalized intensity maps of the range 9,1; 8,2; 9,2; 9,5; 5,2 and Sobel filters showing the directional dependence

that the spatial sampling grid is square, so that the change in amplitude per pixel step is the same in the x and y directions. **Figure 12 shows** the nine normalized intensity values **for the 3×3 square** window.

Figure 13 compares the slope response of selected **range filters with that of the Sobel filters described by equations (11)–(13). The range 9,1 and range 8,2 filters give the same response as the approximate formulations of the Sobel filter that are commonly used. The range 9,5 and 5,1 and range 8,5 and 5,2 filters have half** the response of range 9,1 and range 8,2 **filters and** so are less suitable for slope detection. **Figure 14** shows the directional dependence very **clearly.** The images were produced by filtering an **image** which had a cone-shaped intensity profile. The images have been normalized so that the maximum of the response is 255.

RESPONSE TO A NOISE IMAGE

To determine the noise characteristics of the range filters, an image containing 'pure noise' was filtered. A pure-noise image is generated by assigning to each pixel a random intensity from a prespecified distribution. The mean of the output of the filter gives an indication of the response of the filter to the noise, while the standard deviation gives an indication of the sensitivity of the filter to the noise. If the noise is superimposed on an image of an edge, the mean of the noise response gives an indication of the offset in the threshold used to determine the edge pixels. The standard deviation gives an indication of how readily the background noise may be separated from the edge points. If the standard deviation of the noise response is low, then the sensitivity to the noise is less, enabling the filter to work at lower signal-to-noise ratios. Although exact for linear filters where the superposition principle holds, this reasoning is only an approximation with nonlinear filters such as the range and Sobel filters.

The probability density function for range-filtered pure noise with a range j,i filter using an N element window is given by

$$p(k)=N!\int_{-\infty}^{\infty}\left\{\frac{\left[\int_{-\infty}^{y}p(x)\,\mathrm{d}x\right]^{i-1}}{(i-1)!}\,\frac{\left[\int_{y}^{y+k}p(x)\,\mathrm{d}x\right]^{j-i-1}}{(j-i-1)!}\,\frac{\left[\int_{y+k}^{\infty}p(x)\,\mathrm{d}x\right]^{N-j}}{(N-j)!}\,p(y)p(y+k)\right\}\mathrm{d}y \quad (14)$$

where $p(x)$ is the probability density function of the input noise image. This equation is very difficult, if not impossible, to evaluate analytically for all except the simplest of noise distributions. For uniform noise with zero mean and a standard deviation of σ, equation (14) reduces to

$$p(k)=\frac{N!}{(\sqrt{12}\sigma)^N}\,\frac{k^{j-i-1}}{(j-i-1)!}\,\frac{(\sqrt{12}\sigma-k)^{N-j-i}}{(N-j-i)!}$$

$$0\leqslant k\leqslant\sqrt{12}\sigma \quad (15)$$

This has a mean and variance of

$$\text{mean}=\frac{j-i\sqrt{12}\sigma}{N+1} \quad (16a)$$

$$\text{SD}^2=\frac{12(j-i)(N-j+i+1)\sigma^2}{(N+1)^2(N+2)} \quad (16b)$$

where SD denotes the standard deviation. From equations (15) and (16) it can be seen that, for the uniform distribution, the probability density function of the filtered image depends on the difference in rank values used.

With the Sobel filter of equation (11), computations show the mean and standard deviation to be

$$\text{mean}=1.076\sigma \quad (17a)$$

$$\text{SD}=0.556\sigma \quad (17b)$$

Table 5 lists the means and standard deviations of the resultant images after filtering uniform and gaussian noise images with the range and Sobel filters.

To summarize the results for the range filters and

Table 5. Results of filtering images containing uniform and gaussian noise

Filter	Uniform		Gaussian	
	Mean	SD	Mean	SD
Range 9,1	81.6325	16.1442	87.2969	25.0836
9,2	71.3389	16.8708	71.3885	22.2219
9,3	61.1671	17.0710	60.6002	20.5318
9,4	50.9072	16.8322	51.6382	19.3971
9,5	40.7395	16.0809	43.3224	18.3769
9,6	30.5507	14.7402	35.0725	17.3005
9,7	20.4183	12.7032	26.2316	15.8575
9,8	10.2578	9.4678	15.6757	13.4255
8,1	71.3748	16.8410	71.6212	22.1159
8,2	61.0811	17.0356	55.7128	18.8242
8,3	50.9093	16.7710	44.9244	16.8289
8,4	40.6494	16.0111	35.9625	15.3526
8,5	30.4818	14.6911	27.6467	13.8641
8,6	20.2929	12.6122	19.3968	12.1647
8,7	10.1606	9.3508	10.5558	9.6104
7,1	61.2142	17.0137	61.0654	20.5284
7,2	50.9206	16.7381	45.1570	16.9403
7,3	40.7487	15.9912	34.3686	14.6688
7,4	30.4888	14.6650	25.4067	12.8280
7,5	20.3212	12.6261	17.0909	10.8239
7,6	10.1324	9.3435	8.8409	8.1715
6,1	51.0818	16.7487	52.2244	19.4040
6,2	40.7882	16.0024	36.3160	15.4986
6,3	30.6164	14.7068	25.5277	12.8868
6,4	20.3565	12.6231	16.5657	10.5740
6,5	10.1888	9.3936	8.2500	7.6601
5,1	40.8930	16.0338	43.9745	18.3952
5,2	30.5994	14.7202	28.0661	14.1212
5,3	20.4276	12.6703	17.2777	10.9760
5,4	10.1677	9.3509	8.3158	7.7592
4,1	30.7254	14.7638	35.6587	17.2621
4,2	20.4317	12.7219	19.7503	12.3639
4,3	10.2599	9.4391	8.9619	8.2485
3,1	20.4655	12.6481	26.6968	15.8573
3,2	10.1718	9.3795	10.7884	9.7761
2,1	10.2936	9.4185	15.9084	13.4705
Sobel (11)	32.4027	16.6649	32.0057	17.2996
(12)	20.7953	10.9470	20.4965	11.2633
(13)	29.1935	15.2105	28.9200	15.8923

Input standard deviation is 30.

uniform noise: the mean of the response is proportional to the difference in the rank values used (as given by equation (16)). A rank-position difference of three has approximately the same response as the Sobel filter. The standard deviation varies little over rank-position differences from four to eight, and the value is much the same as that for the Sobel filter. The standard deviation drops steadily for rank-position differences less than four, but (as discussed before) most of these filters are unusable as edge detectors.

When gaussian-distribution noise is used rather than uniform noise, the most notable difference is that the mean and standard deviation of the response are increased if either of the extreme rank positions are used. This is because the extreme rank positions are taken more from the tails of the distribution, and the tails of the gaussian distribution have a lower population density than the tails of the uniform distribution. This results in a larger difference between the rank values, giving a larger mean and standard deviation. When rank positions close to the median position are used, the converse is true. The central region of the gaussian distribution has a higher population density than the uniform distribution, resulting in reduced means and standard deviations.

Using the mean as an indicator, the useful range filters have a larger offset in response than the Sobel filters. The large offsets that arise when extreme rank positions are used may cause problems when detecting edges with lower signal-to-noise ratios. When the standard deviation of the response is used as an indicator of the sensitivity of the filters to noise, there is little difference between the range and Sobel filters.

COMPARISON METHODS

Two methods were used to compare the noise properties of the range filters and the Sobel filters. The first was to measure the number of false detections and false rejections caused by the edge detector, and the other was to use a figure of merit.

The numbers of false detections and false rejections were measured, rather than calculated analytically as suggested by Abdou and Pratt[4]. The test image for this measurement consisted of a series of vertical alternating black and white bands. The bands were spaced in such a way as to give the same number of detected edge and background pixels (10 000 in this case). This image was corrupted by adding noise as specified below and was then processed by the range and Sobel filters. Two intensity histograms were compiled: one of the pixels which would be detected edges in the ideal case, and one of the pixels which would form the background in the ideal case. These histograms were analysed to determine a threshold that minimized the total error. The false detections were the pixels that belonged to the background, but were above the threshold and were detected. The false rejections were the pixels that should have been detected but were not because their intensity was less than the threshold.

With the figure of merit method, the test images contain a single vertical edge 1000 pixels long. This edge image is corrupted by noise in the various ways described below, and then processed by the range and Sobel filters to give the detected edges. The resultant image is thresholded to give an edge map, the threshold being chosen to maximize a figure of merit. The figure of merit (FOM) used is that proposed by Pratt[12]

$$\mathrm{FOM} = \frac{1}{\max(I_a, I_i)} \sum_{i=1}^{I_a} \frac{1}{1+\alpha d_i^2} \tag{18}$$

where I_i is the number of pixels detected in the ideal case; I_a is the number of pixels actually detected; d_i is the distance of the ith detected pixel from the nearest ideally detected pixel; and α is a scaling constant (1/9) which provides a relative penalty between smeared edges and offset edges.

This figure of merit was chosen because other researchers (including Abdou and Pratt[4] and Suciu and Reeves[13]) have used this measure on other edge detection schemes (Sobel, Prewitt, Snyder, Roberts, Kirsch, pixel mass operator, two-level model operators, and compass-gradient methods), and this will permit a direct comparison of results.

EDGE DETECTION IN NOISE

Edge uncertainty measurements

When an edge consists of a broad intensity ramp rather than an infinitesimally narrow border between two regions, the apparent position of the edge can be perturbed by the addition of only a small amount of noise. To test the filters in this situation, uniform noise was added to a slope and the resultant image thresholded. An example of such an image is shown in Figure 15. The uncertainty in the position of the edge is controlled by controlling the amplitude of the added noise. The filters tested are then applied to the edge image, and the figure of merit is calculated for each filter.

Figure 16 shows the figures of merit calculated for the five range filters (range 9,1; 8,2; 7,3; 8,5; 5,1) and the three Sobel filters (from equations (11)–(13)) applied to the test image. All the Sobel filters gave the same figure of merit. The difference in response between the Sobel, range 9,1 and range 5,1 filters is statistically insignificant. A significant improvement in the response is given by the range 8,2 and range 8,5 filters because these filters reject the extreme values. The use of extreme values causes the isolated pixels near the edges of the spread edge to contribute to the detected edge. This results in a wider, more smeared edge with a correspondingly lower figure of merit. The range 7,3 filter shows another significant improvement over the other filters. This improvement again results from the rejection of isolated pixels near the edges. The resultant detected edges for a 12 pixel wide uncertainty are shown in Figure 15.

Point noise

Image point ('salt and pepper') noise is often caused by a noisy sensor or by channel transmission errors[12]. The noise usually affects isolated single pixels by giving

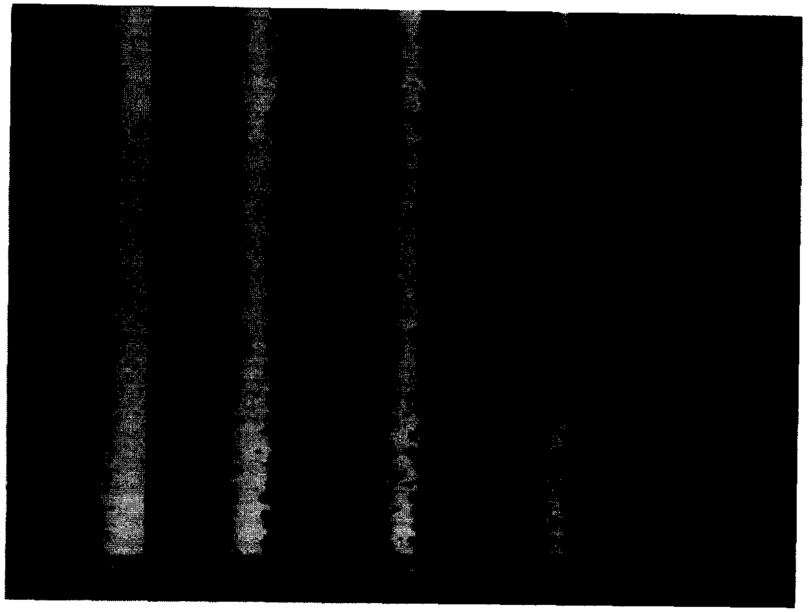

Figure 15. An image containing edge position uncertainty, and the responses after filtering with the range 9,1; 8,2; 7,3 and Sobel filters

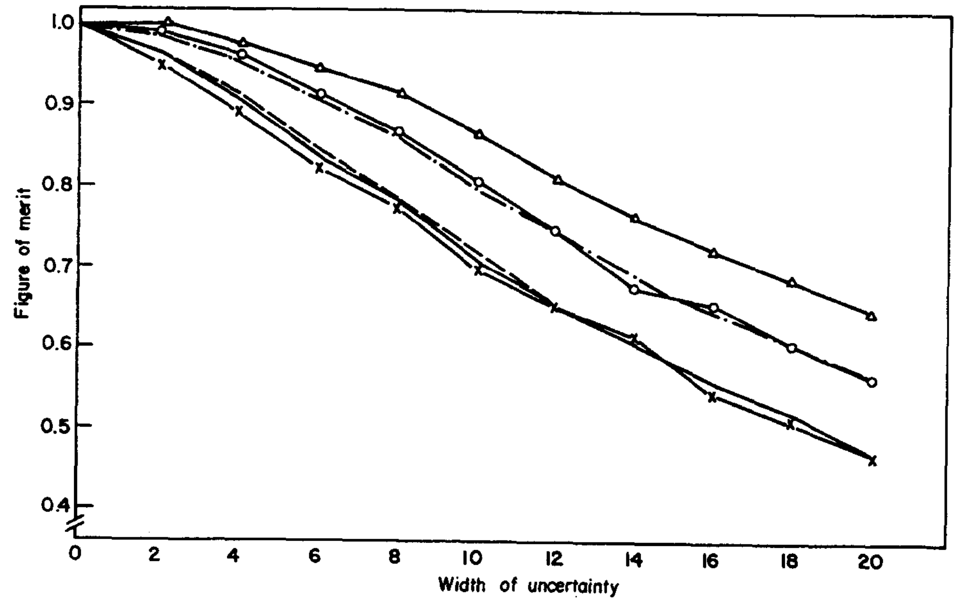

Figure 16. Figures of merit for selected range filters and Sobel filters for different widths of edge uncertainty: ——, Sobel; – – –, range 9,1; –·–, range 8,2; ○—○, range 8,5; ×—×, range 5,1; △—△, range 7,3

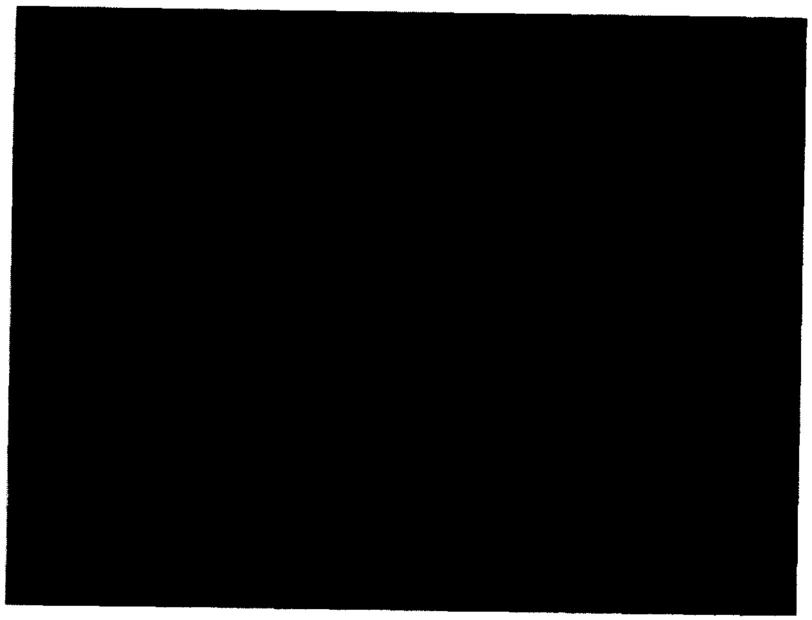

Figure 17. An image containing 1% error rate point noise and the reponses after filtering with the range 9,1; 8,2; 7,3 and Sobel filters

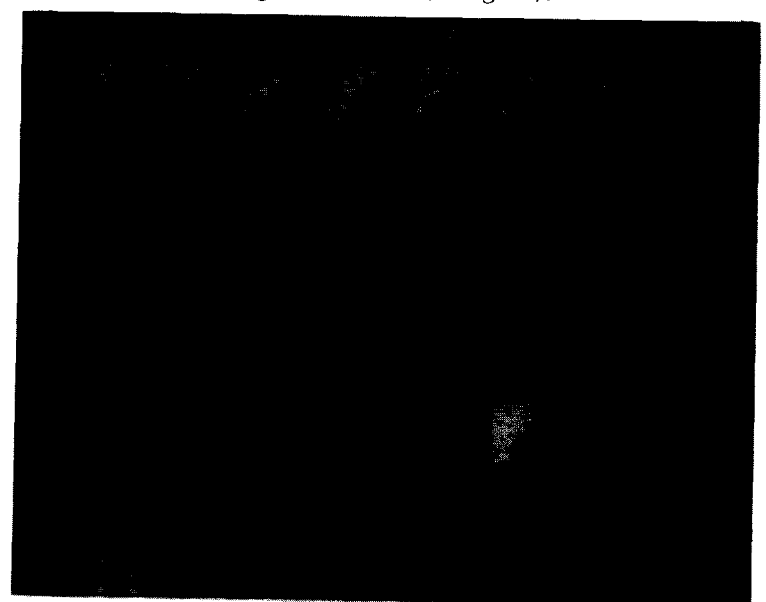

Figure 18. Table of qualitative responses to point noise for the different range filters using a 3×3 window

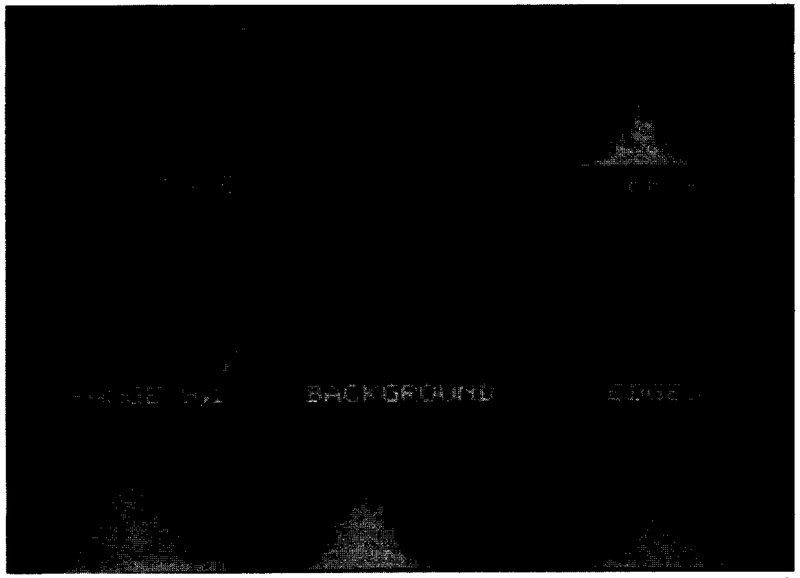

Figure 19. The test image used to determine the proportion of misclassifications when filtering an edge with additive noise. The filtered image is split into its component images, and the histograms of each component are shown

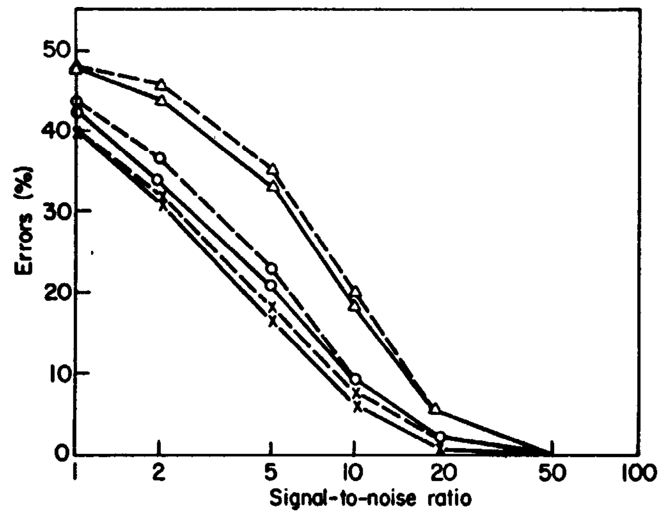

Figure 20. The minimum total misclassification error when filtering an edge corrupted by additive gaussian noise for various signal-to-noise ratios: ×—×, Sobel (11); ×---×, Sobel (12); O—O, range 9,1; O---O, range 8,2; △—△, range 9,5; △---△, range 5,2

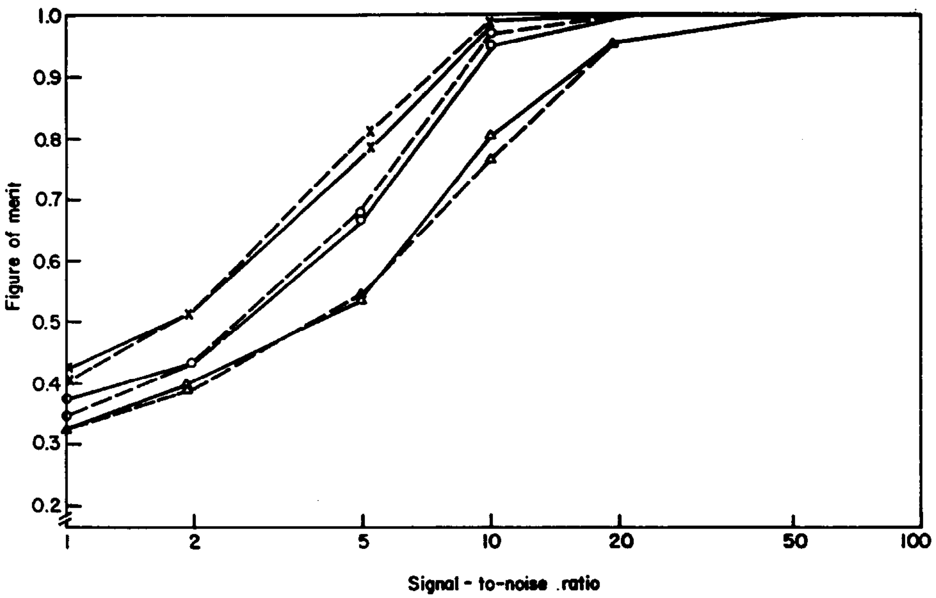

Figure 21. The figure of merit of the resultant detected edge when filtering an edge corrupted by additive gaussian noise for various signal-to-noise ratios (symbols as in Figure 20)

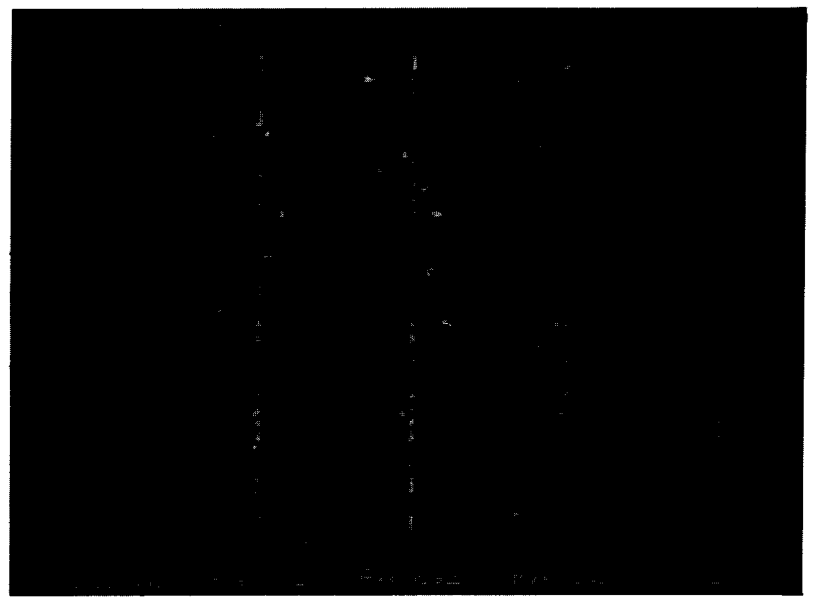

Figure 22. The test image used to determine the figure of merit, and the response of the range 9,1; 8,2; 5,2 and Sobel filters to this test image (SNR=5)

them a markedly different intensity from neighbouring pixels.

To illustrate the effect of point noise on edge detection, consider an image containing an intensity step (height 40) corrupted by simulated binary symmetric channel errors with a bit error rate of 1%. Figure 17 shows the noisy edge image and the results from processing this noisy image by range 9,1 range 8,2 and the Sobel filters. Qualitative results are given for the other range filters in Figure 18. Range filters using the extreme values (ie ranks 1 and 9) are very susceptible to point noise. This is because the noisy pixels often provide the extreme values within the window. When values other than the extremes are used, such noise pixels are rejected, as shown by the response of the range 8,2 filter in Figure 17. The Sobel filters are all susceptible to point noise, but not to the same extent as the range 9.1 filter.

Additive noise

As mentioned previously, because of the nonlinear nature of the range filters, the noise response cannot be added to the edge response to give the total response to noisy edges. For this reason the following tests were carried out. The noisy edges consist of a horizontal step with random gaussian noise added. The signal-to-noise ratio (SNR) is given by

$$\mathrm{SNR} = (h/\sigma)^2 \tag{19}$$

where h is the height of the intensity step and σ is the standard deviation of the gaussian noise.

The first test performed is to determine the number of misclassification errors when thresholding is used to detect the edges after range filtering. Images giving 10 000 detected points and 10 000 background points are filtered, and intensity histograms are compiled of the background and detected points. The histograms are compared and a threshold is chosen to minimize the total number of misclassified pixels. Figure 19 shows part of a typical image, the component images and intensity histograms obtained. Figure 20 plots the total number of errors obtained as a percentage of the total number of pixels for different signal-to-noise ratios. The Sobel filters gave slightly fewer misclassification errors than the range filters using extreme rank positions. Filters using rank positions near the median are considerably more susceptible to the noise. This can be explained by considering the range-filtered image as the difference of the rank-filtered component images. Rank filters using positions close to the median blur edges[5], especially when the edges have a large quantity of noise added to them. This blurring serves to reduce the apparent edge height, resulting in a lower apparent signal-to-noise ratio.

Figure 21 compares the figures of merit of selected range filters with those of the Sobel filters. Figure 22 shows the results obtained with the various filters when the figure of merit was optimized for a signal-to-noise ratio of 5. The figure of merit results show similar trends to the misclassification results, in that the range filters do not perform as well as the Sobel filter at low signal-to-noise ratios. The differences between the different range filters are still apparent, but not as pronounced as with the previous test. A comparison of the results of Figure 21 with those provided by Abdou and Pratt[4] shows that the figure of merit in our test is higher overall. This results from the slightly different shape used for the test image. A relative comparison may still be made between the results.

EFFECT OF WINDOW SHAPE AND SIZE

The noise properties of range filters are much less dependent on the filter shape and size than are the deterministic properties. If the noise is spatially correlated, as will be the case if other filters are used before range filtering, then the window shape will have a greater effect. A full analysis of these more subtle properties of the range filters is beyond the scope of this paper.

SUMMARY AND CONCLUSIONS

In low-noise applications, range filters are considerably more flexible than the Sobel filter. Characteristics of the response that may be 'programmed' include

- the width
- the position relative to the edge
- the connectivity scheme of the output image

When filtering ramp edges, the directional dependence of range filters is the same as that for commonly used approximations to the Sobel filter. Range filters have the disadvantage of providing only the slope magnitudes rather than the complete slope vectors.

When the position of the edge is uncertain, range filters that do not use the extreme rank positions outperform the Sobel filter. This is because the uncertain edge has isolated points along the edge which are ignored by the range filters. With images corrupted by point noise, the noise is ignored by some of the range filters provided that the error rate is low.

The range filters perform adequately when detecting edges corrupted by additive gaussian noise. Where images have been severely corrupted, the Sobel filter performs significantly better than the range filters.

ACKNOWLEDGEMENTS

D G Bailey is supported by a University Grants Committee postgraduate scholarship. The authors gratefully acknowledge the New Zealand Kiwifruit Authority, and the Bay of Plenty Fruitpackers for research funding.

REFERENCES

1 **Castlemen, K R** *Digital image processing* Prentice-Hall, Englewood Cliffs, NJ, USA (1979)

2 **Justusson, B I** 'Median filtering: statistical properties' in **Huang, T S** (ed.) *Two dimensional digital signal processing II, Top. Appl. Phys.* Vol 43 (1981) pp 161–196

3 **Scollar, I, Weidner, B and Huang, T S** 'Image enhancement using the median and interquartile

distance' *Comput. Vision, Graphics Image Process.* Vol 25 (1984) pp 236–251
4 **Abdou, I E and Pratt, W K** 'Quantitative design and evaluation of enhancement/thresholding edge detectors' *Proc. IEEE* (1979) pp 753–763
5 **Hodgson, R M, Bailey, D G, Naylor, M J, Ng, A L M and McNeill, S J** 'Properties, implementaions and applications of rank filters' *Image Vision Comput.* Vol 3 (1985) pp 3–14
6 **Nodes, T A and Gallagher, N C** 'Median filters: some modifications and their properties' *IEEE Trans. Acoust., Speech Signal Process.* Vol 30 (1982) pp 739–746
7 **Goetcherian, V** 'From binary to grey tone image processing using fuzzy logic concepts' *Pattern Recognition* Vol 12 (1980) pp 7–15
8 **Pal, S K and King, R A** 'On edge detection of X-ray images using fuzzy sets' *IEEE Trans. Pattern Anal. Mach. Intell.* Vol 5 (1983) pp 69–77
9 **Duda, R O and Hart, P E** *Pattern classification and scene analysis* Wiley, New York, USA (1973)
10 **Hilditch, C J** 'Linear skeletons from square cupboards' in **Meltzer, B and Mitchie, D** (eds.) *Machine intelligence* University Press, Edinburgh, UK Vol 4 (1969) pp403–420
11 **Freeman, H** 'Computer processing of line drawing images' *ACM Comput. Surv.* Vol 6 (1974) pp 57–97
12 **Pratt, W K** *Digital image processing* Wiley, New York, USA (1978)
13 **Suciu, R E and Reeves, A P** 'A comparison of differential and moment based edge detectors' *Proc. Conf. on Pattern Recognition and Image Processing* (1982) pp 97–102